NANOPRECIPITATES IN STEELS

Joachim H. Schneibel
Oak Ridge National Laboratory, P.O. Box 2008, Oak Ridge, TN 37831-6115
E-mail: schneibeljh@ornl.gov; Telephone: (865) 576-4644; Fax: (865) 574-7659

Bimal K. Kad
University of California-San Diego, 409 University Ctr., Rm 117, La Jolla, CA 92093-0085
E-mail: bkad@ucsd.edu; Telephone: (858) 534-7059; Fax: (858) 534-6373

ABSTRACT

The creep strength of ferritic steels can be substantially improved by the incorporation of a high number density of nano-scale dispersoids. Examples for such alloys are the oxide dispersion strengthened steels MA956, MA957, and PM2000. The dispersoids in these steels contain Y and Ti, or Y and Al. They can be as small as a few nanometers in size. Processing is traditionally carried out by mechanical alloying of elemental or pre-alloyed powders mixed with Y_2O_3 powder. The goal of the present research is to identify alternative ways of producing ultrafine dispersoids. One possible way is internal oxidation, in which reactive elements dissolved in a metallic matrix are selectively oxidized. Internal oxidation experiments were carried out with Fe-Y, Fe-Ti-Y, and Fe-Al-Y precursors. Microstructural analysis showed that dispersoid dimensions as small as 10 nm could be achieved. Atomized Fe-0.25 at% Y powder was internally oxidized and consolidated by hot forging. An increase in the high-temperature creep strength by ~ 20% was observed. Since it is likely that the composition of the precursor alloys is crucial for maximizing the number density and thermal stability of the oxides, experiments allowing the rapid screening of different compositions have been initiated.

INTRODUCTION

Based on a minimum rupture life of 100,000 hours at an applied stress of 100 MPa, the creep strength of ferritic steels used in coal-fired power plants is limited to a temperature of about 620°C (ref. 1). At higher temperatures, the creep life of ferritic steels decreases precipitously. For example, increasing the temperature from 600 to 650°C reduces the creep life of the alloy HCM12A (Fe-11Cr-0.4Mo-2W-0.2V-0.05Nb-0.02Al-0.06N-0.1C, wt%) by a factor of 100 (ref. 2). Higher service temperatures may be obtained with austenitic stainless steels (approximately 690°C) or nickel-base alloys (720°C and above) (ref. 1).

Oxide dispersion strengthened (ODS) steels produced by mechanical alloying of powders followed by hot extrusion are creep- and oxidation-resistant at temperatures well in excess of the maximum temperatures possible for conventional alloys[3]. Klueh et al. showed that the high-temperature creep strength of ODS steels can substantially exceed that of a 9Cr ferritic steel[4]. Ferritic ODS steels contain high number densities of extremely small and stable dispersoids. Kim et al.[5] showed that Ti additions are critical for obtaining nanoclusters with sizes of a few nanometers in a Fe-12Cr-3W-

0.4Ti-0.25Y_2O_3, wt% ("12YWT") ODS steel. Miller et al.'s[6] recent atom probe tomography of MA957 (which has a composition similar to that of 12YWT) showed titanium-, yttrium- and oxygen-enriched particles with diameters on the order of 2-3 nm and number densities on the order of $10^{24}/m^3$. Annealing for 24 hour at 1300°C increased the particle diameters only by a factor of ~3 indicating high thermal stability. It does therefore not come as a surprise that ODS steels are considered as candidate materials for power plant parts such as heat exchanger pipes.

Although ODS steels have high creep strengths, several issues limit their widespread use[3]. The first issue is joining. ODS steels cannot be joined by fusion welding as this destroys the very microstructure giving them their unique properties. Less conventional joining techniques such as plasma-assisted pulsed diffusion bonding and transient liquid phase bonding have recently shown promise[3]. The second issue is the anisotropy in the mechanical properties of these materials. The third issue, which may be the most important, is their high production cost. High cost and the ensuing lack of market penetration are likely to be among the reasons why Plansee GmbH Lechbruck, Germany, has recently discontinued production of its PM2000 alloy.

Ferritic ODS alloys are fabricated by powder-metallurgical (PM) processing involving mechanical alloying of precursor metal or alloy powders with Y_2O_3 powder, followed by consolidation via hot extrusion. The mechanical alloying, which is carried out in a high-energy ball mill, is required to create a uniform dispersion of nanoscale dispersoids. The mechanical alloying approach is expensive and, in addition, difficult to scale up.

Arguably, the most widely used ODS alloy is GlidCop© copper*, which consists of a matrix of pure copper containing an ultrafine dispersion of Al_2O_3 particles ranging in size from 3 to 12 nm with an interparticle spacing of 30 to 100 nm and a particle density of 10^{22} to 10^{23} m^{-3} (ref. 7). Interestingly, GlidCop© copper is not fabricated by mechanical alloying, but by internal oxidation of Cu-Al precursor powders. This suggests that it is worth exploring an internal oxidation route for the processing of ferritic steels. Compared with mechanical alloying, internal oxidation methods are likely to be more economical.

In the present work, results on the internal oxidation of Fe-Y based alloys and intermetallics will be presented. The work is a continuation of previous work on this topic[8,9]. While it is by no means clear at this time whether an internal oxidation route is a realistic alternative to the mechanical alloying of ferritic steels with Y_2O_3 powder we will show that it can produce nanoscale dispersoids with sizes as small as 10 nm. Also, improvements in the high temperature strength due to dispersoid formation by internal oxidation have been demonstrated.

EXPERIMENTAL PROCEDURE

An $Fe_{16}AlY_2$ intermetallic was arc-cast from elemental precursor materials in a partial pressure of argon followed by annealing for 1 hr at 1100°C in vacuum. A coupon of the intermetallic was ground to a 600 grit SiC finish and encapsulated in an evacuated quartz tube together with a mixture of 0.5 g Fe and 0.5 g Fe_2O_3 powders ("Rhines pack"). The powder mixture was placed in one end of the tube and separated from the coupon by a quartz wool barrier. The quartz tube was annealed in order to accomplish the internal oxidation with the partial pressure defined by the Fe-Fe_2O_3 mixture

* Formerly produced by SCM Metal Products, Inc., now produced by North American Höganäs High Alloys LLC.

which causes oxidation of the Al and Y, but not the Fe. The internally oxidized coupon was ground and polished at a glancing angle with respect to its surface in order to increase the apparent width of the internally oxidized zone from ~20-50 μm to ~1 mm. The final polishing was performed with an aqueous solution of colloidal silica.

Argon-atomized Fe-0.25 at% Y powder with a -270 mesh size (≤ 53 μm) and an oxygen concentration of 0.0366 wt% was procured from Crucible Research†. The powder was filled into stainless steel tubes (diameter ~25 mm, wall thickness ~1.5 mm, length ~100 mm) and outgassed by evacuating the tubes while holding them at ~250°C for ~1 hour. Subsequently, the tubes were sealed under vacuum. If internal oxidation was desired, the Fe-0.25 at% Y powder was mixed with an amount of Fe_2O_3 powder sufficient for converting the Y into Y_2O_3. Subsequently, the filled tubes were heat-treated and hot-forged perpendicular to their longitudinal axes, resulting in an oval cross section with a thickness of ~10 mm. Compression specimens with a height of ~5 mm and a diameter of ~3 mm were cut by electro-discharge machining and annealed for 1 hour at 1000°C in vacuum. Polished specimens were examined in a Hitachi S4800 scanning electron microscope (SEM) using secondary and backscattered electron contrast. Conventional powder X-ray diffraction (XRD) was performed. Internally oxidized Fe-0.25 at% Y powder was consolidated and examined by transmission electron microscopy (TEM) in an FEI Tecnai 20 instrument. TEM specimens were prepared by conventional electrolytic twin jet polishing.

Arc-cast Fe-0.8Ti-0.4Y, at% was annealed for 1 day at 1000°C in vacuum and rolled into ~40 μm thick foil. The foil was internally oxidized with a Fe/Fe_2O_3 Rhines pack for 4 days at 800°C and then examined by TEM.

EXPERIMENTAL RESULTS AND DISCUSSION

INTERMETALLIC ALLOYS

Figure 1 shows the thin (as thin as 10 nm) oxide lamellae produced previously[8] in $Fe_{17}Y_2$ by internal oxidation with a Rhines pack for 3 days at 700°C. Figure 2 shows that similar lamellae are produced in $Fe_{16}Al_1Y_2$ that was internally oxidized in the same manner. The lamellae thickness is below 50 nm. As discussed in ref. 8 it is likely that internal oxidation at lower annealing temperatures will result in finer lamellae. The oxide volume fraction is comparable to that of the iron solid solution volume fraction and thus much higher than the oxide volume fraction in ODS alloys, which is typically only a few vol%. ODS alloys synthesized by internal oxidation of intermetallics are therefore not a substitute for typical ODS alloys, but they might have other applications in which high hardness and strength are required.

Fe-0.25 at% Y POWDER

An SEM micrograph of the Fe-0.25 at% Y powder procured from Crucible Research is shown in Fig. 3. Figure 4 shows an SEM micrograph of ODS particles produced by internal oxidation with a

† Crucible Research Center, 6003 Campbells Run Rd., Pittsburgh, PA 15205

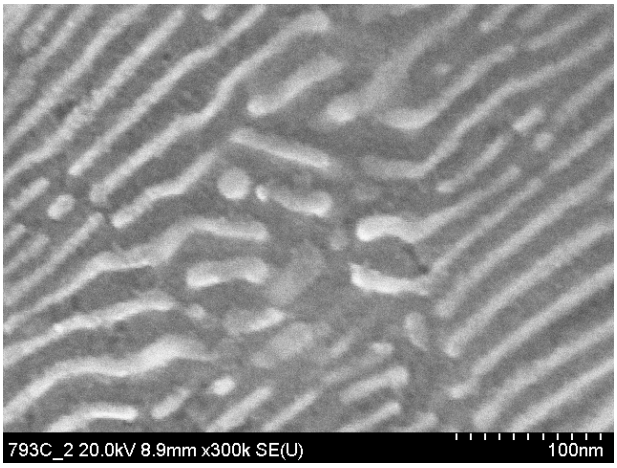

Fig. 1. Y_2O_3 lamellae (bright) produced by internal oxidation of $Fe_{17}Y_2$ with a Fe-Fe_2O_3 Rhines pack for 3 days at 700°C (ref. 8).

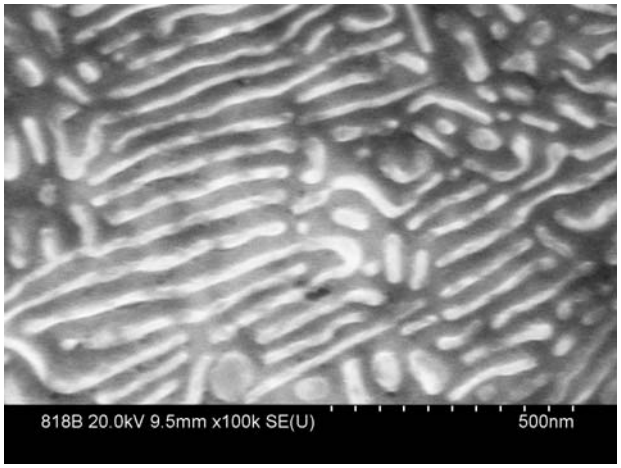

Fig. 2. Oxide particles produced by internal oxidation of $Fe_{16}Al_1Y_2$ with a Fe-Fe_2O_3 Rhines pack for 3 days at 700°C.

Rhines pack for 3 days at 1000°C. The oxide particles are relatively large because of the high annealing temperature. Figure 5 shows a powder XRD pattern of Fe-0.25 at%Y powder mixed with an appropriate amount of Fe_2O_3 powder and annealed for 3 days at 700°C in a covered alumina crucible in vacuum (~10^{-3} Pa). Because of the low volume fraction of the oxide particles, their peaks are barely detectable. The XRD pattern suggests that Y_2O_3, and not the mixed oxide $FeYO_3$, had formed.

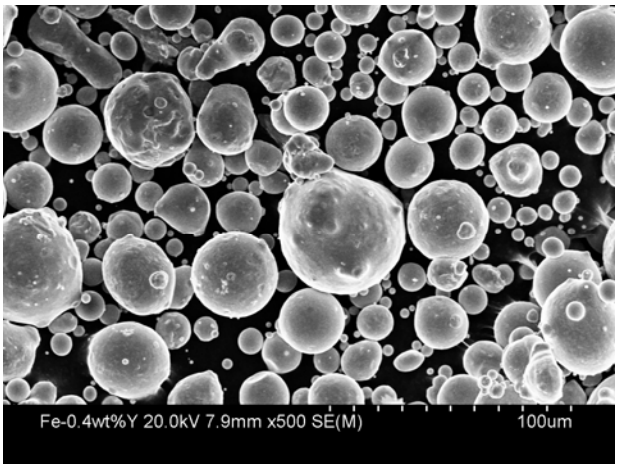

Fig. 3. Argon-atomized Fe-0.25 at% Y powder.

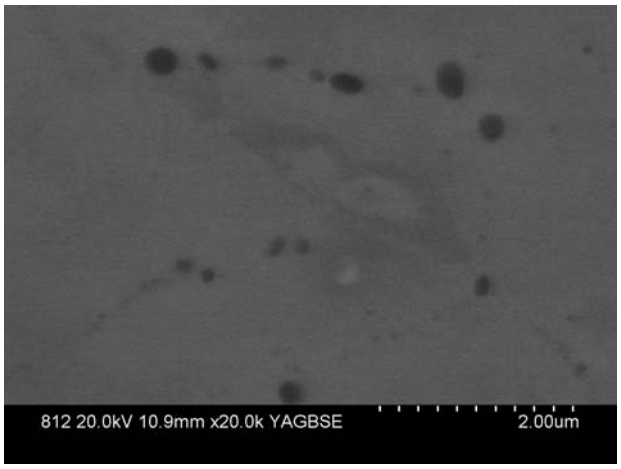

Fig. 4. SEM of cross section through internally oxidized (3 days at 1000°C) Fe-0.25 at%Y particle showing oxide dispersoids.

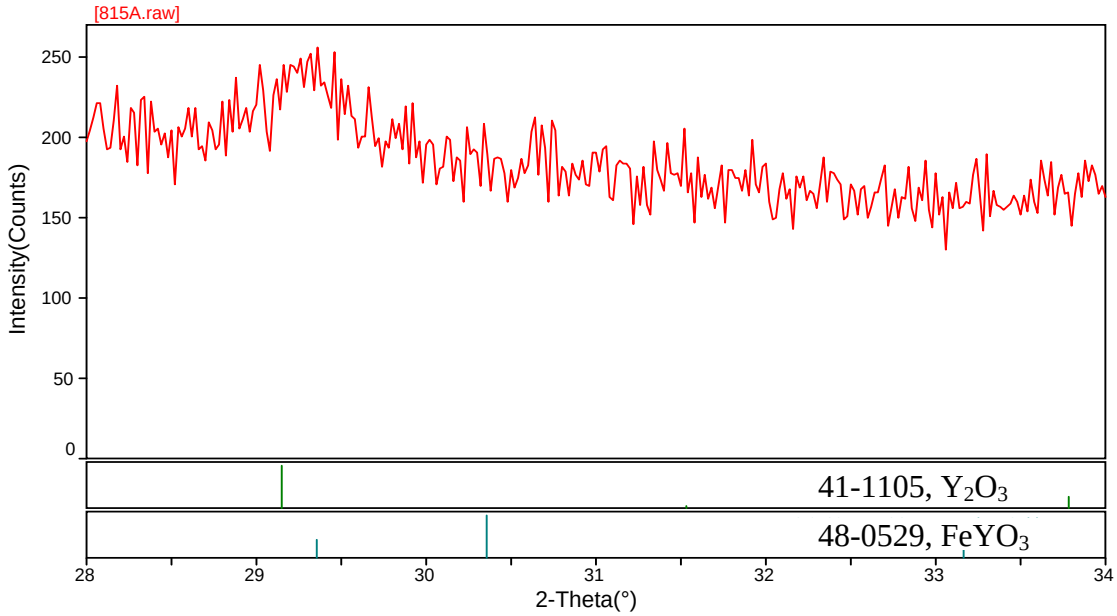

Fig. 5. Powder XRD of Fe-0.25 at%Y powder after annealing with Fe_2O_3 powder for 3 days at 700°C in vacuum.

CONSOLIDATED Fe-0.25 at% Y POWDER

Two batches of Fe-0.25 at% Y powders, one with and one without Fe_2O_3, were vacuum-sealed in stainless steel cans. Both batches were annealed for 3 days at 800°C. For the Fe_2O_3-containing batch, this allowed internal oxidation of the Y with the oxygen supplied by the Fe_2O_3. The batch without Fe_2O_3 powder served as unoxidized reference material. Figures 6 and 7 show stress-strain curves for the reference material and the internally oxidized material tested at room temperature and 800°C. Table 1 lists the room temperature 0.2% offset yield stresses and the true 800°C flow stresses at 5% plastic strain. For both temperatures, the internally oxidized material was slightly stronger. The strengthening likely arises from the formation of Y_2O_3 particles.

Table 1. Comparison of strength values for consolidated Fe-0.25 at% Y powder, with and without internal oxidation.

	0.2% yield stress at room temperature, MPa	True stress at 800°C and 10^{-5} s^{-1} after 5% plastic strain, MPa
Reference Material	153	41
Internally Oxidized	206	49

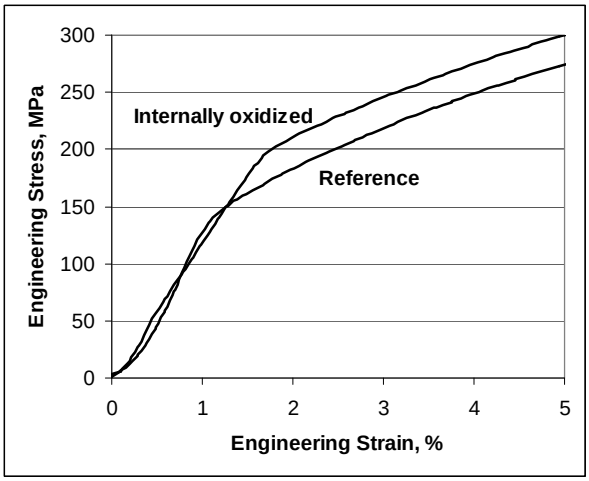

Fig 6: Room temperature stress-strain curves for consolidated Fe-0.25 at%Y with and without internal oxidation.

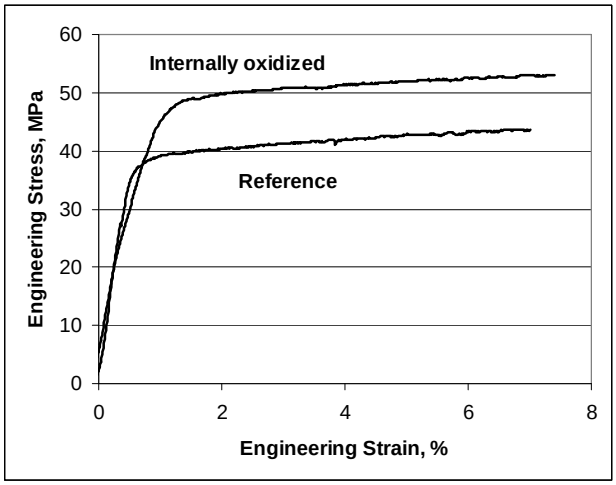

Fig. 7: Stress-strain curves at 800°C and an engineering strain rate of 10^{-5} s^{-1} for consolidated Fe-0.25 at% Y with and without internal oxidation.

Figures 8 and 9 show TEM micrographs of internally oxidized Fe-0.25at% Y after consolidation and annealing for 1 hour at 800°C in vacuum. Figure 8 demonstrates the small size and high number density of the oxide particles. Figure 9, on the other hand, shows the inhomogeneity of the particle distribution. This inhomogeneity may be due to several factors. It may be due to a non-uniform distribution of the yttrium in solid solution, a non-uniform distribution of the added Fe_2O_3 powder, and incomplete penetration of the oxygen into the Fe-Y particles. If a homogeneous particle distribution could be achieved it is conceivable that the strength of the internally oxidized material would be higher than what has been observed in this work.

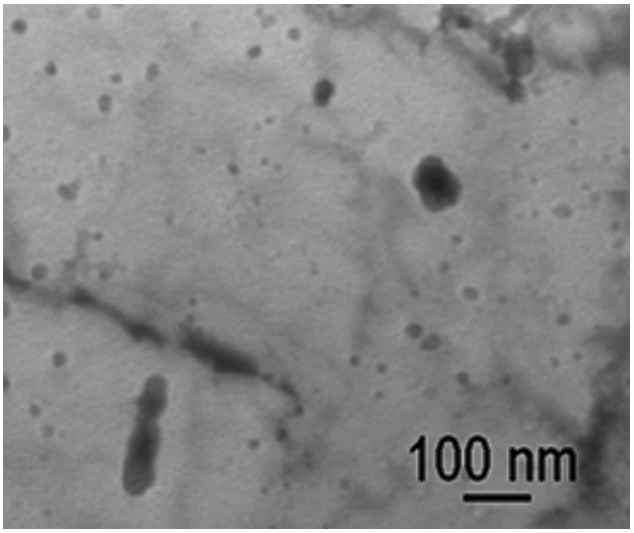

Fig. 8: Particles formed in internally oxidized and compacted Fe-0.25 at% Y powder.

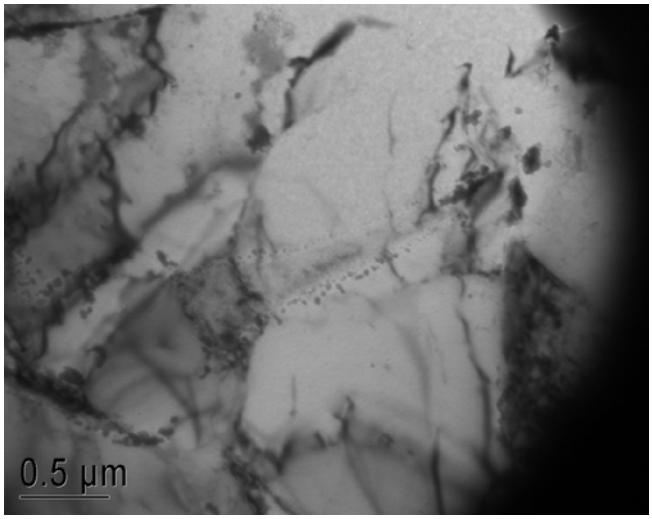

Fig. 9: Inhomogeneous particle distribution in internally oxidized and compacted Fe-0.25 at% Y powder.

SCREENING TESTS FOR DETERMINING THE OPTIMUM COMPOSITION

Research with ODS alloys fabricated using the mechanical alloying process has shown that the composition of the precursor alloy is crucial for obtaining ultra-fine particle sizes. Ukai and Fujiwara[10] determined the average oxide particle size for Fe-12Cr (wt%) based powder that was mechanically alloyed with 0.25 wt% Y_2O_3 powder and hot extruded, to be ~12 nm. When a small concentration of Ti was added (0.8 wt%), the particle size was only ~3 nm. It is conceivable that the composition of the precursor powders is not only important when mechanical alloying is used, but also when the oxide particles are synthesized by internal oxidation. Rapid screening experiments involving internal oxidation followed by TEM examination are therefore needed. One way to screen different alloys rapidly is to arc-cast them, roll them into thin foil (e.g., 50 microns) at room temperature, and then submit them to an internal oxidation anneal. Since the foils are thin, the reactive elements contained in them will become fully oxidized in a reasonable period of time. Figure 10 shows a TEM micrograph of such a foil. The picture is not conclusive because the particle number density is unusually high and because the chemical composition has not been determined. Nevertheless the micrograph does suggest that this approach has merit. Another approach, which has not yet been attempted, would consist of the internal oxidation of bulk alloys to a penetration depth of ~20 to 50 microns, followed by the lift-out of TEM specimens using focused ion beam (FIB) techniques. This approach would have the additional advantage that the mass of the ferromagnetic specimen is very small, which facilitates examination in the TEM.

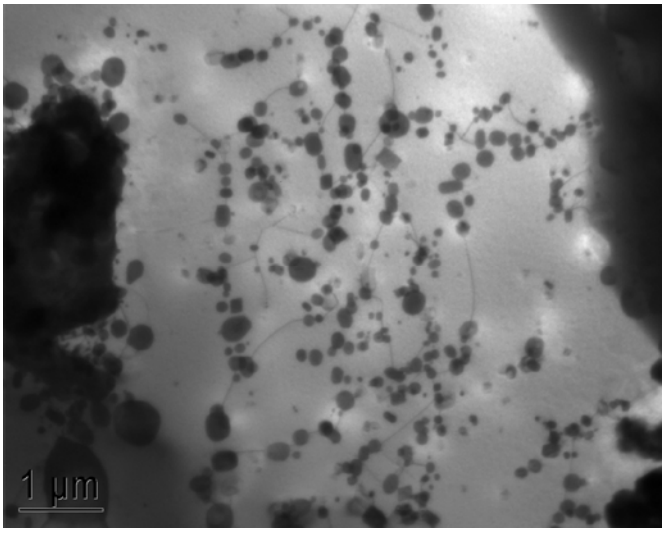

Fig. 10: TEM of internally oxidized (4 days-800°) foil of Fe-0.8Ti-0.4Y, at%.

SUMMARY AND CONCLUSIONS

Internal oxidation experiments were carried out with Fe-Y, Fe-Ti-Y, and Fe-Al-Y alloys and intermetallics. With appropriate heat treatments, oxide particles with dimensions as small as 10 nm were produced. This shows that internal oxidation has the potential to produce ultrafine dispersoids. Consistent with this, the room temperature and high temperature (800°C) strength of Fe-0.25 at% Y was found to increase when the material was internally oxidized prior to testing. Screening tests have been initiated in order to determine the optimum composition of the precursor alloys resulting in the maximum number density of dispersoids with maximum stability.

ACKNOWLEDGEMENTS

This work was sponsored by the Office of Fossil Energy, Advanced Research Materials (ARM) Program, U.S. Department of Energy, under contract DE-AC05-00OR22725 with Oak Ridge National Laboratory managed by UT-Battelle, LLC. A portion of this research was conducted at the SHaRE User Facility, which is sponsored by the Office of Basic Energy Sciences, Division of Scientific User Facilities, U.S. Department of Energy.

REFERENCES

1. J. P. Shingledecker and I. G. Wright, Proceedings of the 8th Liege Conference on Materials for Advanced Power Engineering 2006, Forschungszentrum Jülich GmbH, Germany, 2006, pp. 107-120.
2. B. Nath, E. Metcalfe, and J. Hald, in "Microstructural Development and Stability in High Chromium Ferritic Power Plant Steels," A. Strang and D. J. Gooch, eds., The Institute of Materials, London, England, 1997, pp. 123-143.
3. I. G. Wright, N. S. Bornstein, E. Dyadko, and S. Dryepondt, in "Proceedings of the Twentieth Annual Conference on Fossil Energy Materials," R. R. Judkins, ed., Oak Ridge National Laboratory Report ORNL/4741, Oak Ridge, TN, 2006, pp. 30-38.
4. R. L. Klueh, J. P. Shingledecker, R. W. Swindeman, and D. T. Hoelzer, J. Nuclear Materials 341 (2005) 103-114.
5. I.-S. Kim, B.-Y. Choi, C.-Y. Kang, T. Okuda, P. J. Maziasz, and K. Miyahara, ISIJ International 43 (2003) 1640-1646.
6. M. K. Miller, D. T. Hoelzer, E. A. Kenik, and K. F. Russell, Intermetallics 13 (2005) 387-392.
7. T. S. Srivatsan, N. Narendra and J. D. Troxell, Materials & Design 21[3] (2000) 191-198.
8. J. H. Schneibel, Z. P. Lu, and S. H. Shim, "Nanoprecipitates in Steels, in"Proceedings of the Twenty First Annual Conference on Fossil Energy Materials, April 30-May 2, 2007, published December 2007, R. R. Judkins, ed., url http://www.ms.ornl.gov/fossil/proceedings.shtml, pp. 212-219.
9. J. H. Schneibel and S. Shim, Mater. Sci. and Eng. A488 (2008) 134-138.
10. S. Ukai and M. Fujiwara, J. Nucl. Mat. 307-311 (2002) 749-757.